APPLIED SCIENCES AND ENGINEERING

Microcellular sensing media with ternary transparency states for fast and intuitive identification of unknown liquids

Kyeong Min Song[1], Shinho Kim[2], Sungmin Kang[2], Tae Won Nam[1], Geon Yeong Kim[1], Hunhee Lim[1], Eugene N. Cho[1,3], Kwang Ho Kim[4,5], Se Hun Kwon[5]*, Min Seok Jang[2]*, Yeon Sik Jung[1,3]*

Rapid, accurate, and intuitive detection of unknown liquids is greatly important for various fields such as food and drink safety, management of chemical hazards, manufacturing process monitoring, and so on. Here, we demonstrate a highly responsive and selective transparency-switching medium for on-site, visual identification of various liquids. The light scattering–based sensing medium, which is designed to be composed of polymeric interphase voids and hollow nanoparticles, provides an extremely large transmittance window (>95%) with outstanding selectivity and versatility. This sensing medium features ternary transparency states (transparent, semitransparent, and opaque) when immersed in liquids depending on liquid-polymer interactions and diffusion kinetics. Several different types of these transparency-changing media can be configured into an arrayed platform to discriminate a wide variety of liquids and also quantify their mixing ratios. The outstanding versatility and user friendliness of the sensing platform allow the development of a practical tool for discrimination of diverse organic liquids.

INTRODUCTION

Rapid and accurate identification of organic liquids is increasingly in demand for a wide variety of potential applications such as food and drink inspection, security screening, fuel quality control, synthesis monitoring, and so on (*1*–*5*). Among various candidate technologies, visual detection based on the change in the optical states of sensing materials or devices is attractive, because targets can be distinguished conveniently by the human eye without relying on sophisticated detection systems.

However, previously reported visual sensing methods such as fluorescence or colorimetric signals typically require the use of unconventional small molecules (*6*–*8*), polymers with a complicated monomer backbone (*9*–*11*), or photonic nanostructures composed of complex building blocks (*12*–*16*), which operate through chemical interaction or physisorption between the sensing materials and analyte liquids. Furthermore, many solvatochromic materials have difficulties of dye dissolving in the analyte liquid (*17*) or distinguishing between organic compounds with similar properties (refractive index) (*18*). In addition, in some cases, the resulting visual signals have angle dependency (*19*) or require the use of additional optical spectroscopy to characterize the signals (*13*). These challenges therefore necessitate the development of a new principle that can realize rapid and reliable detection of a broad range of organic liquids.

One potentially practical visual cue that has not been widely explored for detecting organic liquids is a change of transparency. A possible mechanism is to use a light scattering medium that changes its transparency in response to the presence of organic liquids. Although various types of transparency switching in polymeric scattering media in response to external stimuli were reported previously (*20*–*25*), this strategy has yet to be used in practical liquid sensing applications due to fundamental challenges of these materials. For example, simple mixtures of polymers and scattering particles, which can be prepared easily, do not provide a sufficiently strong transparency change to be discernible by human vision, as will be shown in this study. On the other hand, macroporous polymer structures, another example of a responsive light scattering medium, should usually be formed by precisely controlled phase separation of constituents (*26*, *27*), limiting the range of applicable polymers and thus the versatility of liquid identification.

Here, we report ternary-transparency-switching media (TTS media) with an extensive degree of transparency change for fast identification of diverse organic liquids. The TTS media are designed to scatter light through two components, cellular voids and embedded hollow silica particles, to exhibit clear ternary transparency states (transparent, semitransparent, and opaque), depending on the degree of liquid-polymer interaction. Furthermore, we demonstrate that the outstanding versatility of this platform enables the fabrication of an array of TTS media composed of various polymers with controlled thicknesses. TTS medium arrays can therefore differentiate a wide variety of organic liquids, even organic liquids having similar chemical structures and refractive indices, while also being able to quantify the composition of mixture liquids. This work shows that, by systematically engineering the polymeric sensing medium, transparency can be used as a highly effective visual signal for detection of a broad range of organic liquids and that rational design of the transparency-based visual sensor can meet the criteria for a practical sensor.

RESULTS

Designing and fabricating light scattering media with switchable transparency

For transparency change to be used as a practical visual signal, there are three factors that should be considered for designing and

[1]Department of Materials Science and Engineering, Korea Advanced Institute of Science and Technology (KAIST), Daejeon 34141, Republic of Korea. [2]School of Electrical Engineering, Korea Advanced Institute of Science and Technology (KAIST), Daejeon 34141, Republic of Korea. [3]KAIST Institute for NanoCentury, Korea Advanced Institute of Science and Technology (KAIST), 291 Daehak-ro, Yuseong-gu, Daejeon 34141, Republic of Korea. [4]Global Frontier R&D Center for Hybrid Interface Materials (HIM), Busandaehak-ro 63beon-gil, Geumjeong-gu, Busan 609-735, Republic of Korea. [5]School of Materials Science and Engineering, Pusan National University, Busandaehak-ro 63beon-gil, Geumjeong-gu, Busan 609-735, Republic of Korea.
*Corresponding author. Email: sehun@pusan.ac.kr (S.-H.K.); jang.minseok@kaist.ac.kr (M.S.J); ysjung@kaist.ac.kr (Y.S.J.)

engineering sensing media: (i) The medium should be responsive enough to produce a large transparency change to be detectable by the human eye, (ii) the transparency change should be selectively responsive depending on the characteristic of the organic liquids, and (ii) the sensing medium should allow the adoption of a wide range of polymers. If these requirements can be satisfied simultaneously without compromising other factors, then an array platform composed of several different sensing media can be designed. However, as aforementioned, conventional light scattering polymer media based on embedded solid particles or porous structures have critical limitations in the degree of visual signal change and the coverable range of sensing targets.

We therefore designed a new scattering medium containing dual scattering elements—pores and particles—to compose a code-based sensing array with high responsivity and selectivity that can be readily prepared, as depicted in Fig. 1A. This newly designed scattering medium consists of a polymeric matrix composed of cellular pores partially filled with inorganic particles with a wide energy bandgap (>>3 eV) such as silica to minimize light absorption in the visible range.

The dual scattering components, polymer pores and hollow particles, allow the medium to produce a large transparency change in response to the organic liquid. The transparency state of the medium is dependent on the empty or filled state of each component, which is determined by the affinity with the organic liquid, and therefore, the interactions among the polymer matrix, particles, and liquid play a key role for producing multiple transparency states (Fig. 1B). Furthermore, because of the simple structure and facile fabrication process (mixing, casting, and drying), the sensing medium can be built with a variety of polymers, allowing the formation of an array with various porous sensing media that assign a distinctive visual pattern to each organic liquid (Fig. 1C).

The designed sensing medium can be prepared via simple tape casting using a solution containing polymers and inorganic particles, followed by the evaporation of residual solvent. As a result of the solvent evaporation, interphase gaps are created between the polymer matrix and the small particles (Fig. 2A). The interphase gaps are presumed to be derived from the difference in the degree of volumetric change between the polymer matrix and the inorganic particles at the polymer-particle interface during solvent evaporation (Fig. 2B) (*28*–*30*). Because of the removal of the solvent, the organic polymer shrinks in volume, while the volume of the inorganic particles with high rigidity is maintained, leaving behind the gaps.

This gap formation phenomenon is distinguished from other pore formation mechanisms such as nonsolvent-induced phase separation (NIPS) (*26*, *27*), where the pore generation is highly dependent on the solvent systems and/or the presence of water/humidity and is also limited by the type of polymers. Evidence of this is that the porous structures can be formed even in an inert atmosphere, as shown in fig. S1. This suggests that the void formation is not driven by incorporation of water or any components from the environment, which is pivotal to NIPS. Moreover, additional evidence that supports the

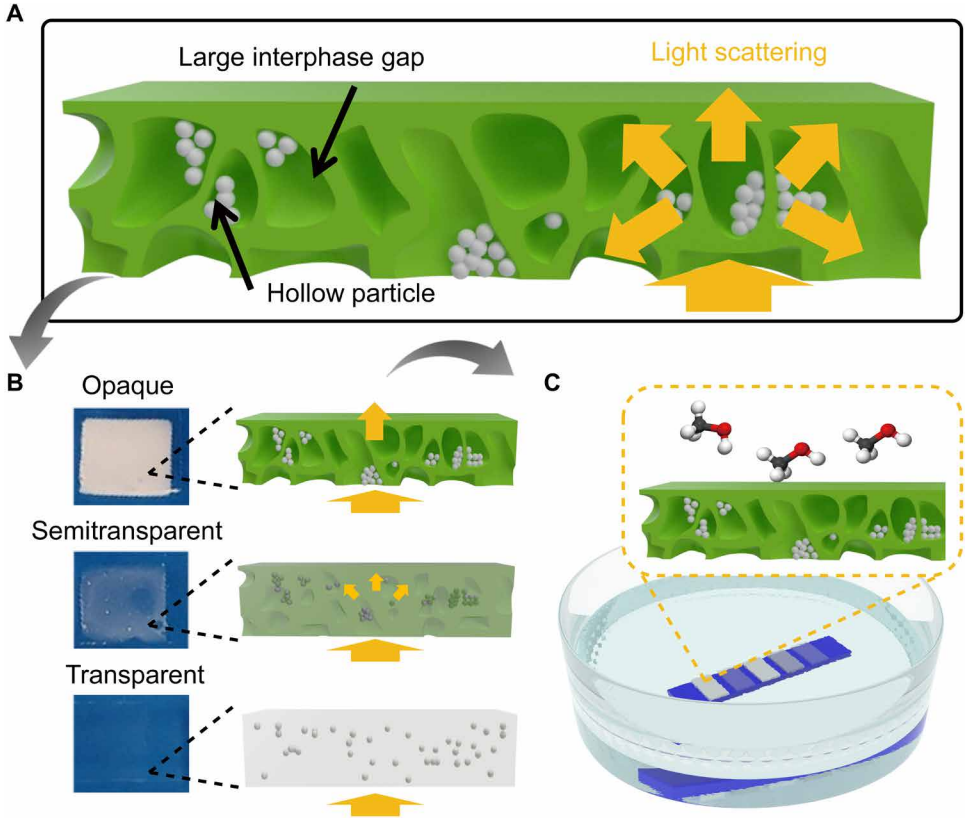

Fig. 1. Design of TSS media for liquid sensing. (**A**) Schematic description of the scattering media with cellular voids and embedded hollow particles at the submillimeter scale. (**B**) Image (left) and schematic (right) of the scattering medium in the three different transparency states (opaque, semitransparent, and transparent). Different arrow sizes indicate the relative intensity of scattered light. (**C**) Illustration of array-based liquid sensing. Photo credit: K. M. Song (KAIST).

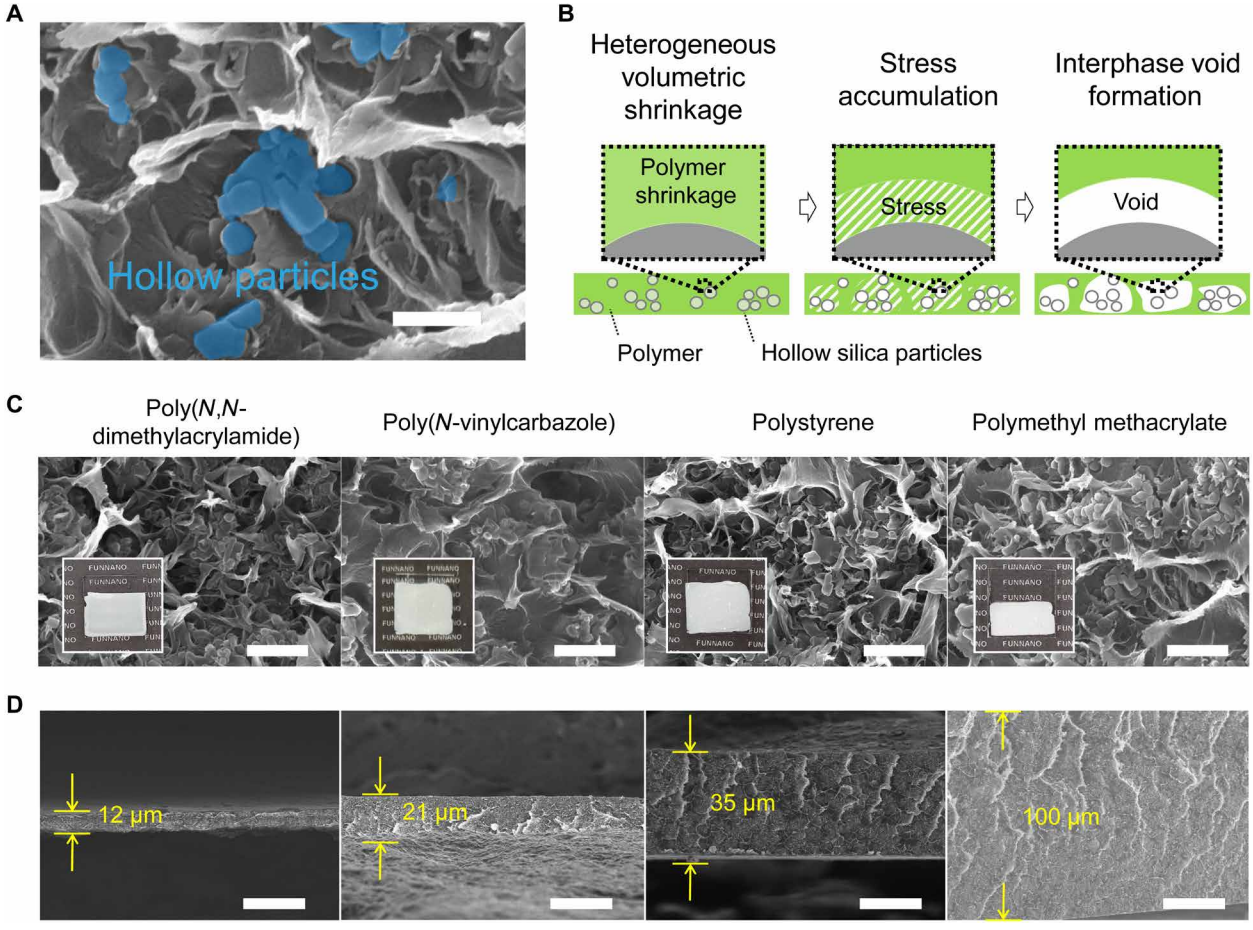

Fig. 2. Design and fabrication of the scattering medium. (**A**) Cross-sectional scanning electron microscopy (SEM) image of the scattering medium with interphase voids and embedded hollow particles (blue colored). (**B**) Schematic of the interphase void formation mechanism in the light scattering media. (**C**) Cross-sectional SEM images of the scattering medium based on poly(*N*,*N*-dimethylacrylamide) (PDMAM), poly(*N*-vinylcarbazole) (PVK), polystyrene (PS), and polymethyl methacrylate (PMMA). Inset: Photo of each scattering film. Scale bars, 1 μm. (**D**) Cross-sectional SEM images of the scattering mediums with different thicknesses: 12, 21, 35, and 100 μm. PMMA is used as a polymer matrix. Scale bars, 25 μm. Photo credit: K. M. Song (KAIST).

pore formation mechanism based on heterogeneous volume shrinkage is the substantial influence of the molecular weight (MW) of the matrix polymer on the pore size, which can be attributed to the different chain reorganization kinetics. This will be discussed in detail in the next section. Last, the porous matrix can be formed using diverse polymers (Fig. 2C) including polymethyl methacrylate (PMMA), polystyrene (PS), poly(*N*-vinylcarbazole) (PVK), and poly(*N*,*N*-dimethylacrylamide) (PDMAM) with varying film thickness from 10 to 100 μm, (Fig. 2D), which is not typically possible with the NIPS mechanism.

Engineering cellular composite media for selective transparency switching

To provide clear visual signals, the light scattering medium needs to maximize the transparency difference upon exposure to the analyte liquid. Ideally, under the atmospheric environment without liquid, the scattering medium should be fully opaque with zero transmittance. When exposed to organic liquids, however, the medium should maintain or change the transparency state, depending on the affinity between the sensing matrix polymer and target liquids. Moreover, from a practical point of view, the change of transparency should be rapid and easily discernible without relying on sophisticated measurement instruments. Therefore, to achieve a maximum transparency difference, we engineered the microstructures of the porous media by controlling the width of interphase gaps and varied the type of embedded particle.

First, we show that the initial opacity of the as-cast polymer composite can be increased to a great extent using a polymer with a sufficiently high MW. The degree of light scattering in the porous medium mainly depends on the interphase gap size, and therefore its systematic control is critical for increasing the initial opacity. This requirement was realized by varying the size of the polymer. For example, PMMA with an MW of ~1000 kg/mol produced a fully opaque film, while the same polymer with a much smaller MW of ~15 kg/mol produced a semitransparent film (Fig. 3A, insets), despite of the same thickness. The scanning electron microscopy (SEM) image (Fig. 3A) of cross-sectional samples confirms that the opacity difference originated from the interphase gap size. For the PMMA (1000 kg/mol), the scattering film has large interphase gaps (300 to 1000 nm) around the hollow particles, whereas in the case of the polymer (15 kg/mol), small (<100 nm) or no gaps were formed around the particles, supporting the dependence of opacity on the gap size.

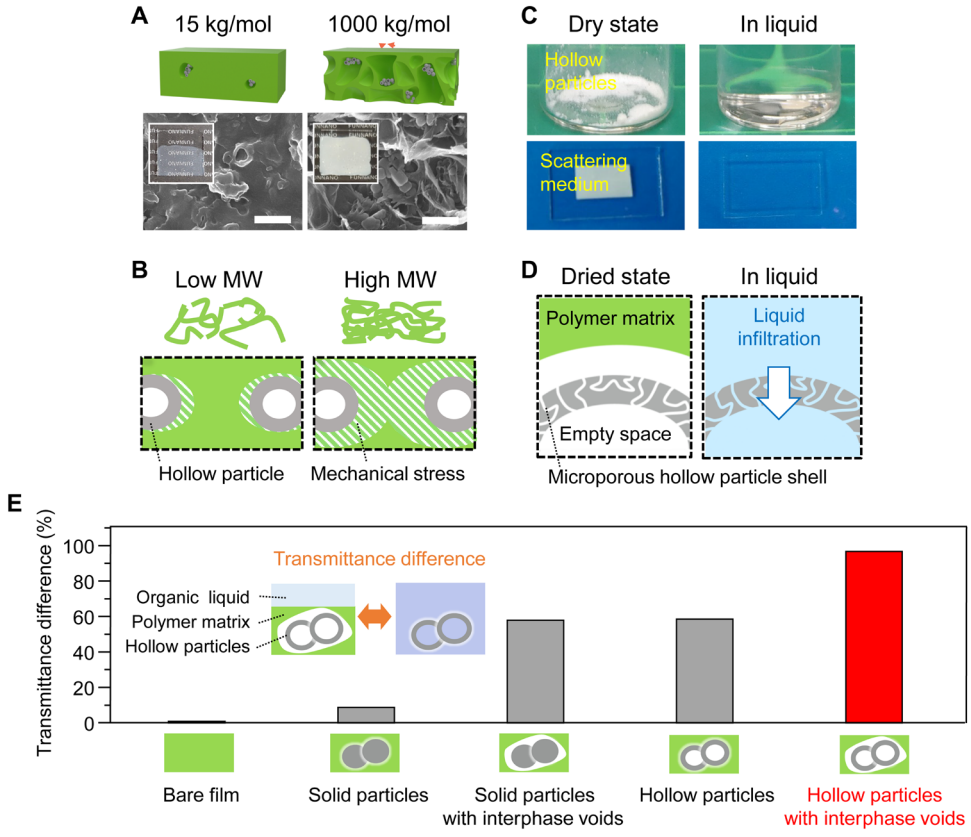

Fig. 3. Optimization of the TSS medium by engineering the width of interphase voids and type of embedded particle. (**A** and **B**) Maximizing the initial opacity of the composite by varying the MW of the polymer. (A) Schematic of the void formation mechanism in the polymer matrix with low (left) and high (right) MW. (B) Schematic and cross-sectional SEM image of the scattering media based on a polymer matrix with 15 kg/mol (left) and 1000 kg/mol (right). Scale bars, 500 nm. Insets are the optical image of each scattering media. (**C** and **D**) Characterization of the hollow particles as an effective light scatterer. (C) Photos of hollow particles (top) and scattering media (bottom) in dried state (left) and after being immersed in liquid (right). (D) Schematic of empty or filling state of hollow particles in dried state (left) and after being immersed in liquid (right). (**E**) Transmittance difference of the scattering medium after being immersed in two different liquids (heptane and chloroform). All scattering films are based on PMMA with identical thickness. Photo credit: K. M. Song (KAIST).

The difference in gap sizes can be explained by the dependence of viscosity on the MW of the polymer chain. According to the Mark-Houwink equation (*31*, *32*), the viscosity of a polymer-solvent system scales with MW$^{\alpha}$, where α ranges between 0.5 and 0.8. Therefore, the viscosity of the polymer (1000 kg/mol) is calculated to be approximately 8 to 28 times higher than that of polymer (15 kg/mol). During the solvent drying of the casted polymer/particle solution, volume shrinkage of the polymer occurs, while the volume of the embedded silica particles is maintained, consequently resulting in a build-up of mechanical stress inside the composite. The built-up mechanical stress can be released through rearrangement of the polymer chain, where, because of their lower viscosity, the smaller MW polymer chains are expected to more rapidly rearrange to fill the shrunk volume. Meanwhile, the higher MW chains move more slowly, resulting in large interphase voids between the polymer matrix and the embedded particles (Fig. 3A) (*28*–*30*).

We now discuss the importance of the type of silica particles. We chose hollow silica particles to act as the second scatterer to widen the transparency switching window of the TTS media. As depicted in Fig. 3C, in the dry state, the hollow particles are fully opaque and behave as a more effective light scatterer due to their internal empty space (*33*) while becoming fully transparent when the organic liquid penetrates the hollow core (*34*). The penetration of the organic liquid into the hollow core is enabled by the presence of the micropores in the shell (*35*), the size of which is sufficient to serve as a passage for the solvent (Fig. 3D) (*36*). In addition, we confirm that the shell of the hollow particles is sufficiently thin to allow liquid penetration into the hollow core (fig. S2). Therefore, when the hollow silica is embedded into the porous media, the media can be fully opaque in the initial state; in contrast, in the presence of a selective range of target liquids, the opaque media can become transparent because of the liquid filling in the interphase gaps and the internal empty space of the hollow silica.

To check the generality of this transparency-switching mechanism, we investigated the transmittance switching behaviors of diverse polymer/particle composites for two organic liquids—chloroform and heptane. The prepared scattering media were pure PMMA, PMMA/solid ZnO particles, PMMA/solid silica particles without interphase voids, PMMA/solid silica particles with interphase voids, PMMA/hollow silica particles without interphase voids, and PMMA/hollow silica particles with interphase voids. Detailed preparation conditions and transmittance graphs of the samples are provided in figs. S3 and S4 and table S1. Compared to other scattering media, the porous media containing both the hollow silica particles and interphase voids generated the largest transparency difference

between the two organic liquids (Fig. 3E). When the scattering film contains only hollow particles or only interphase gaps, the transparency of the composite film changed by about 40 to 60%. Thus, we can conclude that the combined light scattering effect by the interphase voids and hollow particles allow 100% opacity and extensive transparency switching of the scattering medium.

Characterization and elucidation of transparency switching

When the scattering medium is immersed in liquids, the porous sensing medium exhibits ternary transparency states [opaque (0), semitransparent (1), and transparent (2)] depending on the type of liquid. On the basis of this switching behavior, the composite is denoted as a TTS medium. To quantitatively analyze the transparency change of the TTS media, we extracted RGB (red, green, and blue color) values from optical images of the media immersed in liquids (fig. S5) and then converted it into a mean color value (C_{mean}) by the following equation: $C_{mean} = (R_{sensing\ spot} - R_{blank})/R_{blank} + (G_{sensing\ spot} - G_{blank})/G_{blank} + (B_{sensing\ spot} - B_{blank})/B_{blank}$. The C_{mean} values can be used as a metric of transparency when the background color below the liquid-containing vessel is fixed. Figure 4A presents the time-dependent C_{mean} of the TTS media immersed in various organic liquids. Here, the values at 30 s converge clearly to the three groups

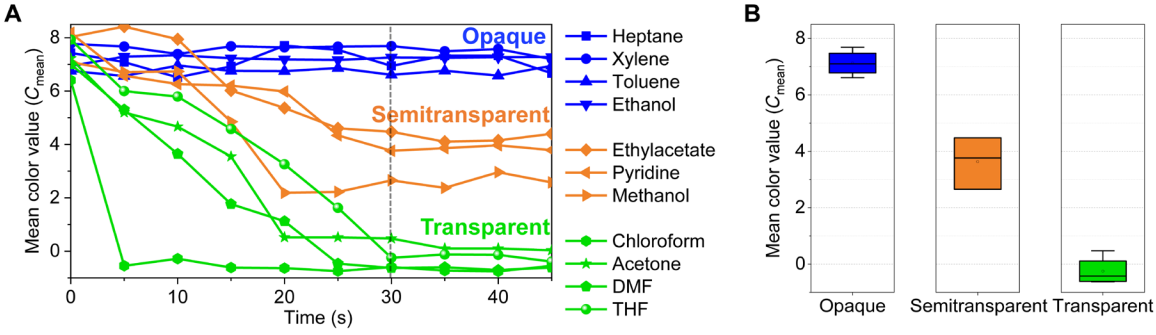

C

Solubility parameter of PMMA = 19 $MPa^{1/2}$

Transparency	Opaque			Semitransparent		Transparent		
Organic liquid	**Heptane**	**Xylene**	**Ethanol**	**Ethyl acetate**	**Methanol**	**Acetone**	**THF**	**Chloroform**
Solubility parameter	15.3	18.2	26.2	18.3	29.7	19.7	18.5	18.7
Molecule shape	Linear	Circular	Linear	Linear	Linear	Linear	Linear	Linear
Molar volume	146.6	119.8	58.4	97.8	40.5	73.5	81.2	80.2
Photograph of sensing media								

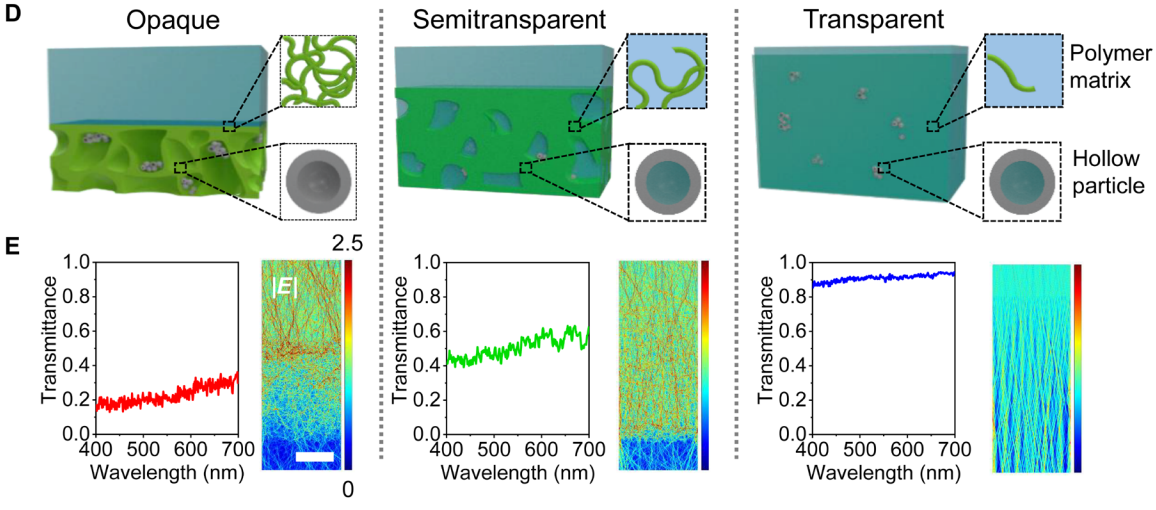

Fig. 4. Transparency switching of the scattering medium. (**A**) The mean color value (C_{mean}) of the images after immersing the scattering medium in diverse organic liquids. Background color is blue. Images are captured every 5 s. DMF, *N*,*N*′-dimethylformamide. (**B**) Distribution of C_{mean} after the scattering medium is exposed to organic liquid for 30 s. (**C**) Different transparency states of the scattering medium according to characteristics of organic liquids. The polymer matrix of the scattering media is based on PMMA. (**D**) The proposed physical models of three different transparency states (opaque, semitransparent, and transparent) after being immersed in organic liquid. The transparency states are dependent on whether the hollow particles and porous polymer structure are empty or filled with a liquid and polymer matrix swells or dissolves. (**E**) Calculated transmittance (left) and electric field distribution (right) of the proposed physical models of three different transparency states. Photo credit: K. M. Song (KAIST).

of transparency depending on the type of organic liquid. Each of these C_{mean} ranges corresponds to each transparency states. [0] opaque: >6, [1] semitransparent: 2 to 5, and [2] transparent: −1 to 1 (Fig. 4B). This accordingly can be used as a criterion for determining the transparency state of the TTS medium.

The transparency of the TTS media immersed in liquid depends on matching of solubility parameters and liquid diffusion kinetics through the polymer matrices; this is determined by several chemical and physical properties of liquids including the chemical affinity between the liquid and the polymer, molecular shape, and molecular size (*37*). For example, as shown in Fig. 4C, the PMMA-based TTS medium demonstrates different transparency states—semitransparent and opaque, respectively, for acetone and xylene, despite their similar solubility parameters. We attribute this phenomenon to the bulky benzene ring of the xylene that can hinder liquid penetration into the polymer matrix (*38*). In addition, methanol, having a different solubility parameter from that of PMMA, renders the TTS medium semitransparent, likely because the extremely small molecular size can greatly expedite the penetration of methanol into the polymer matrix (*39*). Overall, the liquids with superior penetration capability transform the TTS media to be more transparent.

However, observing the microstructural changes of TTS media using microscopy characterization tools is not simple. Alternatively, we prepared several models (Fig. 4D and fig. S6) that can distinguish the different transparency states. Upon penetration of solvent, there will be two possibilities—insoluble (IS) or soluble (S)—regarding the solubility of a polymer for each liquid, as outlined in the following: (state 0) opaque: No liquid penetration, maintaining the highly porous and empty structure of the TTS medium. (State 1-IS) Semitransparent: Partial penetration of liquid causing partial swelling of the polymer without dissolution. Optical scattering is reduced but still exists. (State 1-S) Semitransparent: Partial penetration of liquid with partial dissolution of polymer. Optical scattering is reduced but still exists. (State 2-IS) Substantial penetration of liquid causing full swelling of the polymer without dissolution. Optical scattering is minimized. (State 2-S) Full dissolution of polymer and no optical scattering.

The transmittance of the structure was measured to estimate the transparency state—the transmittance range for each transparency state (fig. S7): opaque (0 to 30%), semitransparent (40 to 70%), and transparent (90% and above). We performed finite-difference time-domain (FDTD) simulations to compare the measured transmittance and calculated transmittance to verify the models. The model structure used in the simulation is a quasi-random pore structure that mimics the key geometric features of the actual structure: a continuous cellular porous structure with an average pore size of 300 to 1000 nm around hollow particles with a diameter of 200 to 400 nm and a shell thickness of 50 nm. For each model, the liquid wetting and filling states of the polymer and the pores were varied. Figure 4E and fig. S8 show that the calculated transmittance of the structure changes depending on whether the polymer matrix is wet or dry state and the pores are filled or empty. In addition, the range of the calculated transmittance matched the experiment results reasonably well, suggesting the validity of the model.

Integrating TTS media as an array for selective liquid identification

Given that the compatibility between the polymer matrix and analyte liquid mainly determines the transparency state of the individual TTS media, different matrix polymers provide corresponding transparency responses to the same liquid (Fig. 5, A and B). Therefore, by arranging a sensing array with various TTS media and designating a code for each transparency state (opaque [0], semitransparent [1], and transparent [2]), the array can generate a unique pattern for each analyte. Theoretically, a sensing array with four TTS media can provide a maximum of 81 pattern combinations, which scales with 3^n, where n is the number of different TTS media in the sensor.

On the basis of the concept of the array-based sensing system, we fabricated a TTS medium array composed of four responsive polymers—PMMA, PVK, PS, and PDMAM—and selectively identified diverse organic liquids. The polymers were selected on the basis of their different polarities so that, depending on the liquid affinity with the polymer matrix, their final transparency states can be determined. Although the fourth component, PVK, has a similar polarity with PS, the larger benzene derivative group makes the dissolution of PVK much slower than that of PS, which helps to differentiate liquid chemicals with similar polarity but with different molecular sizes (*39*). The array starts with a transparency code of 0000 due to their initial opaqueness and demonstrates a distinct transparency pattern for each liquid, which is recorded after 30 s of immersion (Fig. 5C).

We demonstrate that the TTS sensing array can distinguish among benzene homologs, despite that benzene, xylene, anisole, and pyridine have almost the same refractive indices and similar chemical structures, which makes their differentiation extremely challenging by conventional colorimetric sensors or nanoplasmonic sensors. In contrast, in our TTS sensors, each transparency pattern (0220 for benzene, 0120 for xylene, 1121 for anisole, and 1221 for pyridine) for these liquids was distinctly different (Fig. 5C, top middle). For benzene, the PS-based TTS medium exhibited the transparent state due to the strong π-π interaction between the liquid and the polymer, whereas PVK, which contains a bigger benzene derivative, was semitransparent. In contrast, PMMA- and PDMAM-based TTS media remained opaque, which can be explained by their low affinity with benzene. These responses of TTS media toward benzene were analogous to those for xylene except for the PVK-based TTS medium, which showed a semitransparent state due to slower penetration of xylene in PVK, possibly resulting from its slightly larger molecular size than benzene.

For other benzene homologs, the responses of the different TTS media can be similarly explained on the basis of the polymer-liquid interaction and diffusion kinetics. Pyridine and anisole, whose nitrogen or oxygen atoms provide greater hydrophilicity than the simple benzene ring structures, turned PMMA and PDMAM TTS media semitransparent, distinguished from benzene and xylene. Furthermore, because of its relatively large molecule size, anisole leads to more opacity in the PVK medium compared to pyridine. Similarly, the TTS medium array can clearly differentiate alcohols, including methanol (1002), ethylene glycol (0002), butanol (1001), and ethanol (0001) by exhibiting unique patterns for each target liquid (Fig. 5C, top right). In addition, in addition to the homologs, other liquids with similar physical nature were also distinguishable, such as amyl acetate and tetrahydrofuran (THF), which have an identical refractive index of 1.4 (Fig 5C, bottom left).

The sensing specificity can be further improved by adding the time parameter (t) in the analysis of acquired sensing patterns (Fig. 5D). Taking anisole and chlorobenzene as examples, although they showed a similar transparency code pattern (1121) at t = 30 s, chlorobenzene turned the PMMA medium into the transparent state much faster.

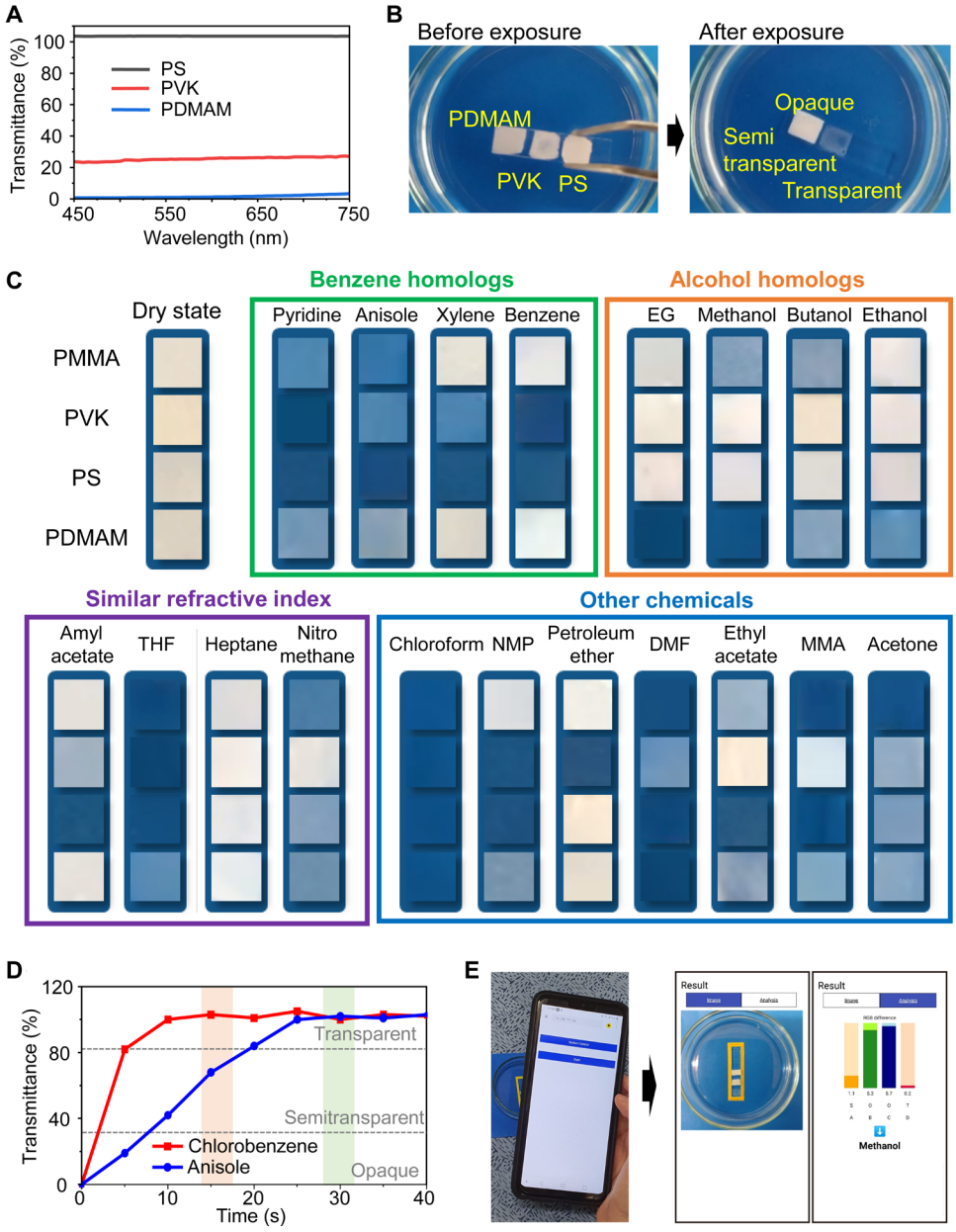

Fig. 5. Integration of the scattering mediums for liquid sensing. (**A**) Transmittance graph of the scattering films with three different polymers after being immersed in same organic liquid (xylene). (**B**) Image of scattering medium array before (left) and after (right) being immersed in organic liquid. The array is composed of three different responsive polymers (PDMAM, PVK, and PS). (**C**) Table of transparency patterns for different series of organic liquids. Background of the array is blue. The images are taken after immersing the array in the liquid for 30 s. Inset figures are the refractive index of each liquid. EG, ethylene glycol. (**D**) Transmittance changes of the scattering medium as a function of exposure time to chlorobenzene and anisole. The polymer matrix of the scattering media is based on PMMA. (**E**) Smartphone-based transparency analysis system for liquid identification. Photo credit: K. M. Song (KAIST).

Therefore, as depicted in fig. S9, their pattern codes were distinguishable at 15 s, showing a transparency pattern of 0121 and 1121, respectively. In addition, even highly viscous liquids can also be identified with the current sensing system within reasonably short time (30 s) via thickness control of the scattering film (fig. S10).

For more facile identification of unknown liquids based on the code pattern, we developed a smartphone application that can automatically determine TTS sensing code patterns and identify the liquids from a preestablished database. As shown in Fig. 5E, the application automatically recognized the array pattern, successfully matched their RGB values with the reference values stored in the database, and, as an example, immediately identified the unknown liquid as methanol. The types of TTS media, the number of patterns in the device, and the range of detectable liquids in the application can be extended without limitations, suggesting that the transparency-switching platform can be used as an easy-to-use visual sensor for the general public.

Characterizing the composition of liquid mixtures using thickness-varied arrays

Characterizing the mixing ratio of constituent components in a liquid mixture remains a challenge with previous liquid detection principles (*13*). In this study, we demonstrate quantification of the mixing ratio using another parameter—the thickness of TTS media, as illustrated in Fig. 6A. In the case of two-component mixtures, where one component interacts actively with the polymer matrix and the other does not, the range of sensing medium thickness for transparency change can be monitored to estimate the mixing ratio. More specifically, when the sensing material is sufficiently thin, a small amount of penetrated liquid is sufficient to affect the whole polymer matrix in a short immersion time, and the opaque sensing film thus becomes transparent even with a low target concentration, while a thick sensing medium remains almost opaque for the same time period of immersion. Then, on the basis of this thickness-dependent transparency change in each analyte concentration, an array integrated by sensing materials with different thicknesses is expected to generate a distinct pattern for each target concentration and, as a result, can be used to identify the unknown analyte concentration in a liquid.

Using this strategy, we designed a sensing system that can quantify the relative fraction of two liquids with very similar physical and chemical characteristics. Chloroform and xylene were chosen as target analytes, because they have close solubility parameters (18.7 and 18.2, respectively) and refractive indices (1.44 and 1.49, respectively) that are difficult to distinguish by conventional sensing techniques. The matrix polymer used was PMMA, which becomes transparent in chloroform while remaining opaque in xylene. The observed transparency states of PMMA-based TTS media with a variable film thickness for different liquid compositions are illustrated in Fig. 6B. With increasing chloroform fraction, the maximum thickness (th_{max}) of the transparent and semitransparent films increased linearly with good repeatability [relative standard deviation (RSTD), <15%; error bars in fig. S11A], demonstrating the ability of the sensing array to successfully estimate the concentration of chlorobenzene.

Furthermore, this approach is also effective for three-component mixtures based on two types of TTS media with varied thicknesses. As a demonstration, we investigated the relationship between the relative fraction of water, methanol, and toluene in mixtures and the transparency status of PDMAM- and PS-based TTS media that have selective affinity with methanol and toluene, respectively. The th_{max} shows a linear increase and decrease respectively for PS and PDMAM media with an elevating fraction of toluene (Fig. 6, C and D, and fig. S11, C and D), depending on the individual affinity of the liquids with the polymers. In particular, th_{max} of PDMAM media shows a small RSTD (<15%), demonstrating good repeatability (fig. S11B). This further confirms that the TTS medium platform is highly feasible for identifying the composition in a multicomponent liquid.

To demonstrate the practicality of the TTS medium array, we applied the array to a real-life application for identifying methanol poisoned liquors. Methanol, a toxic chemical, is a natural by-product during ethanol production and is often found in fatal amounts in

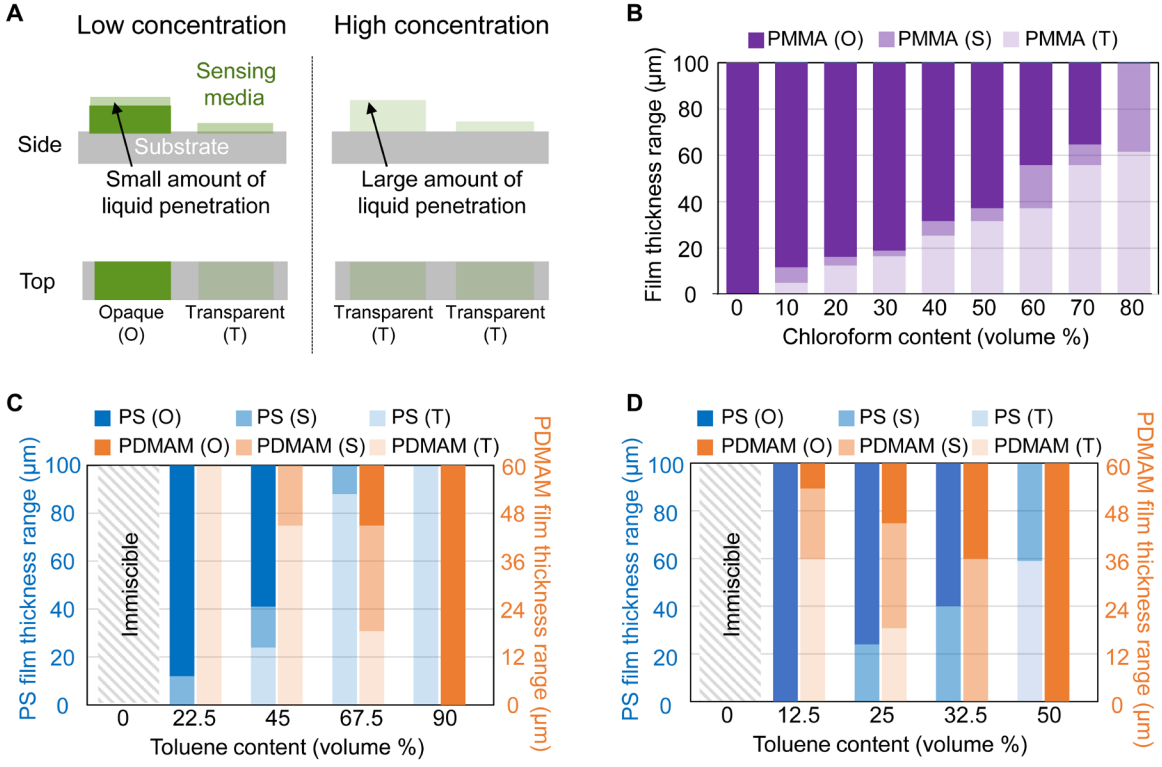

Fig. 6. Identifying composition of the liquid mixture by controlling the thickness of TTS media. (**A**) Schematic of principle for detecting the liquid mixture ratio using film thickness as a parameter. (**B**) Transparency states of the scattering medium as a function of target liquid concentration (*x* axis) and film thickness (*y* axis). (**C** and **D**) Transparency states of the scattering medium in the three-component mixture. The organic liquids in the system include methanol, toluene, and heptane. Heptane concentration is fixed at (C) 10 weight % (wt %) and (D) 50 wt %. Opaque, semitransparent, and transparent are denoted as O, S, and T, respectively.

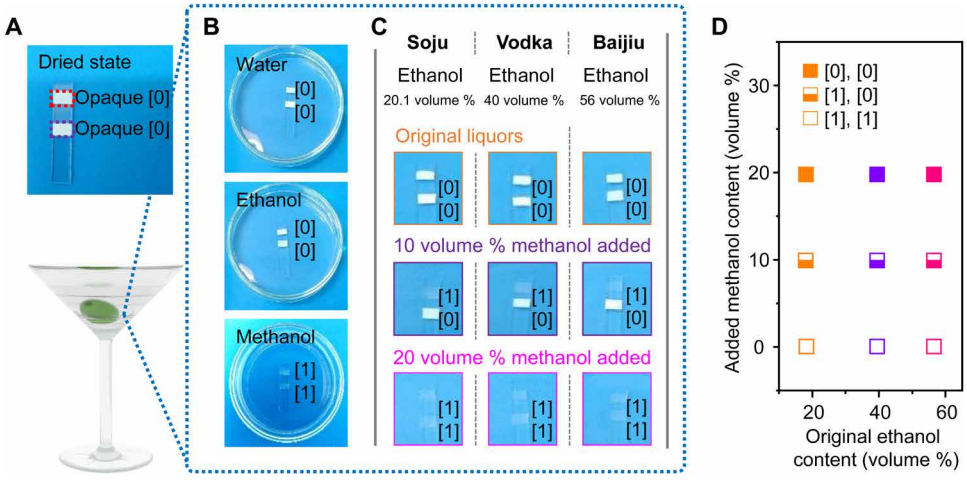

Fig. 7. Differentiation of pure and laced liquors. (**A** to **C**) Photographs of an array before (A) and after being immersed in control liquids (B) and in alcohols (C) for 30 s. The array is composed of PMMA-based TTS media, and the thickness of each sensing spot is 16 (dotted red box) and 27 μm (dotted purple box). Opaque, semitransparent, and transparent are coded as 0, 1, and 2, respectively. (**D**) Transparency patterns of the array as a function of original ethanol content (*x* axis) and added methanol content (*y* axis). Photo credit: K. M. Song (KAIST).

homebrewed liquors or illegal alcoholic beverages, leading to hundreds of victims in many countries (*40*, *41*). Conventional visual sensing methods have difficulty in distinguishing between chemically similar alcohols (methanol and ethanol), let alone the concentration, due to cross-interferences between the two types of alcohol (*42*, *43*).

As a solution, we designed TTS media through thickness variation and careful polymer selection for detecting and quantifying methanol within the liquor mixture. The array is composed of PMMA-based TTS media with a thickness of 16 and 27 μm (Fig. 7A). PMMA was selected as the polymer due to the fast diffusion rate of methanol molecules compared to ethanol and water into the PMMA matrix (*39*), and therefore, it selectively responds to methanol and becomes semitransparent in methanol while remaining opaque in water and ethanol (Figs. 4D and 7B). For the standard liquor, soju (20.1 volume % of ethanol, Chamisul Classic, a popular liquor in South Korea), vodka (40 volume % of ethanol; Absolut Vodka), and baijiu (56 volume % of ethanol; Erguotou, a popular liquor in China) were used, while laced liquors were prepared by adding 10 and 20 volume % of methanol into the original liquor. As depicted in Fig. 7 (C and D), the TTS medium array showed a clear response to methanol and methanol-mixed liquors while being independent of liquor type and ethanol concentration. These results indicate that a thickness-tuned TTS medium array with a properly selected polymer matrix is able to detect methanol and its content in liquors without interference of ethanol, thus demonstrating its potential to be used as a simple method to screen methanol-contaminated alcohols.

DISCUSSION

In summary, we demonstrated a TTS media–based visual sensor for fast and facile detection of diverse organic liquids. The sensing process can be directly performed in liquid phases, which has been challenging for many existing colorimetric sensors due to their intrinsic limits of sensing materials. Various types of TTS media were successfully prepared via simple polymer/particle blending and solvent evaporation. TTS media were designed to accommodate dual scattering components—embedded hollow particles and microcellular pores surrounding the particles, which are formed by heterogeneous volume shrinkage of the polymer matrix during solvent evaporation. Unlike conventional polymer-based light scatterers, the combination of microcellular pores and embedded hollow particles in the TTS media enabled a wide transparency switching window and clear ternary (transparent, semitransparent, and opaque) transparency states that are easily distinguishable by the human eye. The transparency change of the TTS media was explained by liquid filling of the scattering components, which is determined by the degree of polymer-liquid interaction and diffusion dynamics. Furthermore, the TTS media allow the adoption of various polymers and therefore can be arranged into an array sensor composed of different polymer matrices with controlled thickness that gives a unique code combination (0 for opaque, 1 for semitransparent, and 2 for transparent) to each organic liquid. Using the code pattern of the visual sensor, it was demonstrated that even analogous liquids with highly similar molecular structures and refractive indices can be successfully discriminated. In addition, the TTS sensor can also be used to estimate the composition of liquid mixtures by checking the thickness range of TTS media that generates distinct transparency states depending on the liquid mixture compositions. Despite its limitation in identifying colored liquids and detecting trace amounts of target liquids in a mixture, the TTS media afford outstanding customizability. This suggests that this new transparency switching sensor could provide a versatile liquid identification tool for many practical applications such as oil quality control, environment surveillance, and food and drink safety.

MATERIALS AND METHODS

Experimental design

Materials

Silicon wafer [P type (B), (100); T = 280 μm; MADE LAB] and optical slide glass (T = 1000 μm; Marienfeld) were used as the substrates for the sensing medium. Hollow silica particles were obtained from Illsin Co. PMMA (Mn = 1000 kg/mol; Sigma-Aldrich), PS (Mn = 1200 kg/mol; Polymer Source), PDMAM (Mn = 900 kg/mol; Polymer

Source), and PVK (Mn = 1100 kg/mol; Sigma-Aldrich) were used as received. All organic liquids were purchased from Sigma-Aldrich and were used as received: benzene (>99.9%), toluene (>99.9%), chloroform (>99.9%), *N*,*N*′-dimethylformamide (>99.9%), methanol (>99.9%), ethanol (>99.9%), acetone (>99.9%), xylene (>99.9%), heptane (>99.9%), THF (>99.9%), dimethyl sulfoxide (>99.9%), dioxane (>99.9%), isopropyl alcohol (>99.9%), ethyl acetate, and methyl methacrylate (99%; Sigma-Aldrich). Vodka (40 volume % of ethanol; Absolut Vodka, Sweden), soju (20.1 volume % of ethanol; Chamisul Classic, South Korea), and baijiu (56 volume % of ethanol; Erguotou, China) were used as testing liquors.

Preparation of TTS media

The TTS media were fabricated as follows. The polymer-hollow particle solution was prepared by dissolving 10 weight % (wt %) polymer and 1 wt % hollow particle in the designated solvent and stirred for 5 hours. Detailed conditions for the polymer/hollow particle solution are described in tables S1 and S2. Slide glass was used as the substrate for the TTS media and was washed in the order of deionized water, isopropyl alcohol, and acetone, followed by ultraviolet (UV)/ozone treatment for 30 min. After the cleaning procedure, the substrate was taped to form the desired pattern. The prepared solution was then deposited onto the taped substrate using a doctor blade. After the solvent was fully dried, the tape was gently removed, leaving behind the TTS media in the desired pattern. The array was fabricated by repeating the same process with different polymer/hollow particle solutions.

Characterization

Cross-sectional images of TTS media were obtained by SEM (S-4800, Hitachi) with an acceleration voltage of 10 kV and a working distance of 5 mm. Images of hollow particles were obtained by transmission electron microscopy (Tecnai G2 F30 S-Twin, FEI) with an acceleration voltage of 300 kV. Transmittance was measured by a UV–visible spectrophotometer (Mecasys, OPTIZEN POP, Korea) with reference to a bare substrate immersed in a liquid-filled glass dish. RGB values from the photograph were extracted by ImageJ.

Statistical analysis

FDTD simulation

Commercial FDTD (Lumerical FDTD) software was used to calculate the light transmission of polymer films. The transmission of the films was calculated for a plane wave injected into the periodic two-dimensional structure with dimensions of 40 μm by 30 μm. The refractive indices of SiO_2, methanol, heptane, and chloroform were set as 1.475, 1.32, 1.38, and 1.45, respectively. The refractive indices of PMMA films were different depending on the swelling states, i.e., 1.42 and 1.49 for swollen and nonswollen films, respectively.

Smartphone-based sensing system

The number of sensing spots and the polymer types can be set upon starting the application. A TTS medium array immersed in an unknown liquid for 30 s was captured and was analyzed by an application using the following algorithm. The location of each sensing spot on the array was identified, followed by extraction of the average RGB values from each of the sensing spot. The extracted RGB values were then converted into a mean color value (C_{mean}) by the following equation: $C_{mean} = (R_{sensing\ spot} - R_{blank})/R_{blank} + (G_{sensing\ spot} - G_{blank})/G_{blank} + (B_{sensing\ spot} - B_{blank})/B_{blank}$. For the application to differentiate between the transparency states, the C_{mean} range was designated for each transparency state: opaque, >6; semitransparent, 2 to 5; transparent, −1 to 1. Measuring the transparency state using C_{mean} showed low color variation between the samples. The resulting transparency states of the array were then matched with the database, identifying and displaying the unknown liquid in the application window.

SUPPLEMENTARY MATERIALS

Supplementary material for this article is available at https://science.org/doi/10.1126/sciadv.abg8013

REFERENCES AND NOTES

1. L. Zhu, D. Meier, Z. Boger, C. Montgomery, S. Semancik, D. L. DeVoe, Integrated microfluidic gas sensor for detection of volatile organic compounds in water. *Sens. Actuators B* **121**, 679–688 (2007).
2. E. D. Tsamis, J. N. Avaritsiotis, Design of planar capacitive type sensor for "water content" monitoring in a production line. *Sens. Actuators A Phys.* **118**, 202–211 (2005).
3. M. A. Kessler, J. G. Gailer, O. S. Wolfbeis, Optical sensor for on-line determination of solvent mixtures based on a fluorescent solvent polarity probe. *Sens. Actuators B* **3**, 267–272 (1991).
4. M. Bunge, N. Araghipour, T. Mikoviny, J. Dunkl, R. Schnitzhofer, A. Hansel, F. Schinner, A. Wisthaler, R. Margesin, T. D. Märk, On-line monitoring of microbial volatile metabolites by proton transfer reaction-mass spectrometry. *Appl. Environ. Microbiol.* **74**, 2179–2186 (2008).
5. M. Bai, W. R. Seitz, A fiber optic sensor for water in organic solvents based on polymer swelling. *Talanta* **41**, 993–999 (1994).
6. S. H. Lim, L. Feng, J. W. Kemling, C. J. Musto, K. S. Suslick, An optoelectronic nose for the detection of toxic gases. *Nat. Chem.* **1**, 562–567 (2009).
7. L. Chen, J. W. Ye, H. P. Wang, M. Pan, S. Y. Yin, Z. W. Wei, L. Y. Zhang, K. Wu, Y. N. Fan, C. Y. Su, Ultrafast water sensing and thermal imaging by a metal-organic framework with switchable luminescence. *Nat. Commun.* **8**, 15985 (2017).
8. N. A. Rakow, K. S. Suslick, A colorimetric sensor array for odour visualization. *Nature* **406**, 710–713 (2000).
9. H. N. Kim, Z. Guo, W. Zhu, J. Yoon, H. Tian, Recent progress on polymer-based fluorescent and colorimetric chemosensors. *Chem. Soc. Rev.* **40**, 79–93 (2011).
10. G. Das, B. P. Biswal, S. Kandambeth, V. Venkatesh, G. Kaur, M. Addicoat, T. Heine, S. Verma, R. Banerjee, Chemical sensing in two dimensional porous covalent organic nanosheets. *Chem. Sci.* **6**, 3931–3939 (2015).
11. X. Jiang, H. Gao, X. Zhang, J. Pang, Y. Li, K. Li, Y. Wu, S. Li, J. Zhu, Y. Wei, L. Jiang, Highly-sensitive optical organic vapor sensor through polymeric swelling induced variation of fluorescent intensity. *Nat. Commun.* **9**, 3799 (2018).
12. Y. Zhang, J. Qiu, R. Hu, P. Li, L. Gao, L. Heng, B. Z. Tang, L. Jiang, A visual and organic vapor sensitive photonic crystal sensor consisting of polymer-infiltrated SiO2 inverse opal. *Phys. Chem. Chem. Phys.* **17**, 9651–9658 (2015).
13. Y. Zhang, Q. Fu, J. Ge, Photonic sensing of organic solvents through geometric study of dynamic reflection spectrum. *Nat. Commun.* **6**, 7510 (2015).
14. Y. Yang, H. Kim, J. Xu, M. S. Hwang, D. Tian, K. Wang, L. Zhang, Y. Liao, H. G. Park, G. R. Yi, X. Xie, J. Zhu, Responsive block copolymer photonic microspheres. *Adv. Mater.* **30**, 1707344 (2018).
15. K. Szendrei, P. Ganter, O. Sànchez-Sobrado, R. Eger, A. Kuhn, B. V. Lotsch, Touchless optical finger motion tracking based on 2D nanosheets with giant moisture responsiveness. *Adv. Mater.* **27**, 6341–6348 (2015).
16. R. A. Potyrailo, R. K. Bonam, J. G. Hartley, T. A. Starkey, P. Vukusic, M. Vasudev, T. Bunning, R. R. Naik, Z. Tang, M. A. Palacios, M. Larsen, L. A. Le Tarte, J. C. Grande, S. Zhong, T. Deng, Towards outperforming conventional sensor arrays with fabricated individual photonic vapour sensors inspired by *Morpho* butterflies. *Nat. Commun.* **6**, 7959 (2015).
17. J. R. Askim, M. Mahmoudi, K. S. Suslick, Optical sensor arrays for chemical sensing: The optoelectronic nose. *Chem. Soc. Rev.* **42**, 8649–8682 (2013).
18. C. F. Blanford, R. C. Schroden, M. Al-daous, A. Stein, Tuning solvent-dependent color changes of three-dimensionally ordered macroporous (3DOM) materials through compositional and geometric modifications. *Adv. Mater.* **13**, 26–29 (2001).
19. L. He, M. Janner, Q. Lu, M. Wang, H. Ma, Y. Yin, Magnetochromatic thin-film microplates. *Adv. Mater.* **27**, 86–92 (2015).
20. J. Zhang, G. Pu, M. R. Dubay, Y. Zhao, S. J. Severtson, Repositionable pressure-sensitive adhesive possessing thermal-stimuli switchable transparency. *J. Mater. Chem. C.* **1**, 1080–1086 (2013).
21. M. Weng, L. Chen, P. Zhou, J. Li, Z. Huang, W. Zhang, Low-voltage-driven, flexible and durable paraffin-polydimethylsiloxane-based composite film with switchable transparency. *Chem. Eng. J.* **295**, 295–300 (2016).
22. J. Y. Park, H. Song, T. Kim, J. W. Suk, T. J. Kang, D. Jung, Y. H. Kim, PDMS-paraffin/graphene laminated films with electrothermally switchable haze. *Carbon N. Y.* **96**, 805–811 (2016).

23. J. Mandal, M. Jia, A. Overvig, Y. Fu, E. Che, N. Yu, Y. Yang, Porous polymers with switchable optical transmittance for optical and thermal regulation. *Joule* **3**, 3088–3099 (2019).
24. K. Manabe, T. Matsubayashi, M. Tenjimbayashi, T. Moriya, Y. Tsuge, K. H. Kyung, S. Shiratori, Controllable broadband optical transparency and wettability switching of temperature-activated solid/liquid-infused nanofibrous membranes. *ACS Nano* **10**, 9387–9396 (2016).
25. H. N. Apostoleris, M. Chiesa, M. Stefancich, Improved transparency switching in paraffin-PDMS composites. *J. Mater. Chem. C.* **3**, 1371–1377 (2015).
26. S. Yoo, J. H. Kim, M. Shin, H. Park, J. H. Kim, S. Y. Lee, S. Park, Hierarchical multiscale hyperporous block copolymer membranes via tunable dual-phase separation. *Sci. Adv.* **1**, e1500101 (2015).
27. R. Wei, J. Guo, L. Jin, C. He, Y. Xie, X. Zhang, W. Zhao, C. Zhao, Vapor induced phase separation towards anion–/near-infrared-responsive pore channels for switchable anti-fouling membranes. *J. Mater. Chem. A* **8**, 8934–8948 (2020).
28. S. Takahashi, D. R. Paul, Gas permeation in poly(ether imide) nanocomposite membranes based on surface-treated silica. Part 2: With chemical coupling to matrix. *Polymer* **47**, 7535–7547 (2006).
29. R. C. Cammarata, Surface and interface stress effects in thin films. *Prog. Surf. Sci.* **46**, 1–38 (1994).
30. M. A. Aroon, A. F. Ismail, T. Matsuura, M. M. Montazer-Rahmati, Performance studies of mixed matrix membranes for gas separation: A review. *Sep. Purif. Technol.* **75**, 229–242 (2010).
31. K. Wang, H. Huang, J. Sheng, Determination of the Mark-Houwink equation parameters and their interrelationship. *J. Liq. Chromatogr. Relat. Technol.* **21**, 1457–1470 (1998).
32. H. L. Wagner, The Mark–Houwink–Sakurada equation for the viscosity of atactic polystyrene. *J. Phys. Chem. Ref. Data.* **14**, 1101–1106 (1985).
33. W. Suthabanditpong, C. Takai, M. Fuji, R. Buntem, T. Shirai, Improved optical properties of silica/UV-cured polymer composite films made of hollow silica nanoparticles with a hierarchical structure for light diffuser film applications. *Phys. Chem. Chem. Phys.* **18**, 16293–16301 (2016).
34. L. Ernawati, T. Ogi, R. Balgis, K. Okuyama, M. Stucki, S. C. Hess, W. J. Stark, Hollow silica as an optically transparent and thermally insulating polymer additive. *Langmuir* **32**, 338–345 (2016).
35. M. N. Gorsd, L. R. Pizzio, M. N. Blanco, Synthesis and characterization of hollow silica spheres. *Procedia Mater. Sci.* **8**, 567–576 (2015).
36. V. M. Masalov, N. S. Sukhinina, E. A. Kudrenko, G. A. Emelchenko, Mechanism of formation and nanostructure of Stöber silica particles. *Nanotechnology* **22**, 275718 (2011).
37. C. M. Hansen, *Hansen Solubility Parameters: A User's Handbook* (CRC Press, ed. 2, 2007).
38. H. L. Frisch, "Diffusion in polymers" edited by J. Crank and GS Park, Academic Press, London and New York, 1968; 452 pg. *J. Appl. Polym. Sci.* **14**, 1657 (1970).
39. N. L. Thomas, A. H. Windle, Diffusion mechanics of the system PMMA-methanol. *Polymer* **22**, 627–639 (1981).
40. P. Pressman, R. Clemens, S. Sahu, A. W. Hayes, A review of methanol poisoning: A crisis beyond ocular toxicology. *Cutan. Ocul. Toxicol.* **39**, 173–179 (2020).
41. M. Shokoohi, N. Nasiri, H. Sharifi, S. Baral, S. Stranges, A syndemic of COVID-19 and methanol poisoning in Iran: Time for Iran to consider alcohol use as a public health challenge? *Alcohol* **87**, 25–27 (2020).
42. Z. Jin, H. He, H. Zhao, T. Borjigin, F. Sun, D. Zhang, G. Zhu, A luminescent metal-organic framework for sensing methanol in ethanol solution. *Dalton Trans.* **42**, 13335–13338 (2013).
43. J. van den Broek, S. Abegg, S. E. Pratsinis, A. T. Güntner, Highly selective detection of methanol over ethanol by a handheld gas sensor. *Nat. Commun.* **10**, 4220 (2019).

Acknowledgments: We thank S. U. Shin at the KAIST Analysis Center for Research Advancement for advice in obtaining and analyzing Fourier transform infrared spectra. **Funding:** This work was supported by the Global Frontier Hybrid Interface Materials (GFHIM) program of the National Research Foundation of Korea (NRF) funded by the Ministry of Science, ICT and Future Planning (no. 2013M3A6B1078874) **Author contributions:** K.M.S. and Y.S.J. conceived the project and designed the experiments. K.M.S. conducted most of the fabrication and the analysis of experiments. S.Kim and M.S.J. discussed and conducted FDTD simulations. S.Kang developed the transparency analysis application for a smart phone. T.W.N. and G.Y.K. contributed to the transmittance analysis. H.L. contributed to the SEM analysis. K.M.S., E.N.C., K.H.K., S.-H.K., and Y.S.J. wrote most of the manuscript. All authors discussed the results and contributed to the final manuscript. **Competing interests:** Y.S.J. is an inventor on a patent related to this work filed by Korea Advanced Institute of Science and Technology and R&D Center for Hybrid Interface Materials (no. KR 10-2257093-1000, filed 18 September 2019, published 21 May 2021). The authors declare that they have no other competing interests. **Data and materials availability:** All data needed to evaluate the conclusions in the paper are present in the paper and/or the Supplementary Materials.

Submitted 28 January 2021
Accepted 22 July 2021
Published 15 September 2021
10.1126/sciadv.abg8013

Citation: K. M. Song, S. Kim, S. Kang, T. W. Nam, G. Y. Kim, H. Lim, E. N. Cho, K. H. Kim, S.-H. Kwon, M. S. Jang, Y. S. Jung, Microcellular sensing media with ternary transparency states for fast and intuitive identification of unknown liquids. *Sci. Adv.* **7**, eabg8013 (2021).